Investigation of the Local Lattice Structure and the Effects of the Orbital Reduction Factor on the *g* Factors of a Trigonal $[Ni(H_2O)_6]^{2+}$ Cluster in $NiTiF_6 \cdot 6H_2O$ and $ZnSiF_6 \cdot 6H_2O$ Crystals at Different Temperatures

Hui-Fang Li[a], Xiao-Yu Kuang[a,b], Huai-Qian Wang[a], and Ai-Jie Mao[a]

[a] Institute of Atomic and Molecular Physics, Sichuan University, Chengdu 610065, China
[b] International Centre for Materials Physics, Academia Sinica, Shenyang 110016, China

Reprint requests to H.-F. L.; E-mail: scu_kxy@163.com

Z. Naturforsch. **63a,** 609 – 615 (2008); received March 10, 2008

The local octahedral environment of Ni^{2+} in $NiTiF_6 \cdot 6H_2O$ and $ZnSiF_6 \cdot 6H_2O$ crystals with a trigonal distortion has been studied at different temperatures, based on the complete energy matrices. The calculated results showed that the local lattice structure around an octahedral Ni^{2+} centre in $NiTiF_6 \cdot 6H_2O$ and $ZnSiF_6 \cdot 6H_2O$ exhibits a compression distortion. Simultaneously, the orbital reduction effect on the *g* factors has been studied. The relationship between $\Delta g = g_\parallel - g_\perp$ and orbital reduction factor *k* at 4.2, 77 and 298 (302) K has been discussed, suggesting that there is an almost linear relation between *k* and Δg for the Ni^{2+} ion in $NiTiF_6 \cdot 6H_2O$ and $ZnSiF_6 \cdot 6H_2O$ at each temperature.

Key words: Local Structure; Orbital Reduction Effect; EPR Spectrum; Complete Energy Matrices.

1. Introduction

Nickel fluorotitanate hexahydrate ($NiTiF_6 \cdot 6H_2O$) and zinc fluorosilicate hexahydrate ($ZnSiF_6 \cdot 6H_2O$) belong to the series of compounds having the general formula $M(II)X(IV)F_6 \cdot 6H_2O$ with M = Zn, Ni, Mg, Co, Fe and X = Si, Ti, Sn, Zr. The fluorosilicates and fluorotitanates have a trigonally distorted CsCl-type structure including the two complex ions: the hydrated metal complex $[M(H_2O)]^{2+}$ and the silicon (or titanium) hexafluoride ion $[XF_6]^{2-}$. Since Pauling [1] has determined the structure in the space group $R\bar{3}$ for $NiSnCl_6 \cdot 6H_2O$, this local structure symmetry was assumed to be typical of the fluorosilicate and fluorotitanate hexahydrate series. Many physicists and chemists have been devoted to studying these compounds. For instance, the zero-field splitting (ZFS) parameter *D* and *g* factors ($g_\parallel, g_\perp$) for $NiTiF_6 \cdot 6H_2O$ crystals at different temperatures have been reported by Rubins et al. [2]. The first EPR studies of pair spectra were made on Ni^{2+} pairs in $ZnSiF_6 \cdot 6H_2O$ by Al'tshuler and Valishev [3]. These results provide important information to further studies of the transition metal Ni^{2+} ion. The EPR parameters and the temperature dependence of *D* for Ni^{2+} in $ZnSiF_6 \cdot 6H_2O$ crystals were measured [4 – 7]. The magnitude of $\partial D/\partial T$ has a maximum of (0.0027 ± 0.0001) cm^{-1}/K, decreasing to about 0.0015 cm^{-1}/K at room temperature [5]. However, no theoretical considerations of the effect of temperature on the local structure and the orbital reduction effect on the *g* factors for Ni^{2+} in $NiTiF_6 \cdot 6H_2O$ and $ZnSiF_6 \cdot 6H_2O$ crystals have been performed. In this paper, the local structure parameters *R* and θ at different temperatures are determined by simulating the EPR and optical spectra based on the complete energy matrices for a d^8 ion in a trigonal ligand-field. Meanwhile, by considering the orbital reduction effect, the relationship between the orbital reduction factor *k* and Δg has been discussed.

2. Theory

The spin Hamiltonian, including the ZFS and Zeeman terms, can be written as [8]

$$\hat{H}_S = g_\parallel \beta H_z S_z + \beta g_\perp (H_x S_x + H_y S_y) + D\left(S_z^2 - \frac{1}{3}S(S+1)\right). \quad (1)$$

From the spin Hamiltonian, the ZFS parameter *D* can be calculated by the splitting energy levels in the ground state $^3\mathrm{A}_2$ for a zero magnetic field:

$$\begin{aligned} &E(\pm 1) = \frac{1}{3}D, \quad E(0) = -\frac{2}{3}D, \\ &\Delta E = E(\pm 1) - E(0) = D. \end{aligned} \tag{2}$$

For Ni^{2+} in $\mathrm{NiTiF_6 \cdot 6H_2O}$ and $\mathrm{ZnSiF_6 \cdot 6H_2O}$ the structure symmetry of the water octahedron surrounding Ni^{2+} belongs to the $R\bar{3}$ space group. The perturbation Hamiltonian for a d^8 Ni^{2+} ion in this system can be written as [9]

$$\begin{aligned} \hat{H} &= \hat{H}_{\mathrm{ee}} + \hat{H}_{\mathrm{SO}} + \hat{H}_{\mathrm{LF}} + \hat{H}_{\mathrm{Zeeman}} \\ &= \sum_{i<j} \frac{e^2}{r_{i,j}} + \zeta \sum_i l_i s_i + \sum_i V_i \\ &\quad + \sum_i \mu_{\mathrm{B}} (k\vec{l}_i + g_{\mathrm{e}} \vec{s}_i) \cdot \vec{H}, \end{aligned} \tag{3}$$

where $\hat{H}_{\mathrm{ee}}$ is the electron-electron repulsion interaction, $\hat{H}_{\mathrm{SO}}$ is the spin-orbit coupling interaction, $\hat{H}_{\mathrm{LF}}$ is the ligand-field interaction, $\hat{H}_{\mathrm{Zeeman}}$ is the Zeeman interaction, V_i is the ligand-field potential, and k ($0.5 < k \leq 1$) is the orbital reduction factor [10]. The ligand-field potential V_i may be expressed as

$$\begin{aligned} V_i = \gamma_{00} Z_{00} &+ \gamma_{20} r_i^2 Z_{20}(\theta_i, \varphi_i) + \gamma_{40} r_i^4 Z_{40}(\theta_i, \varphi_i) \\ &+ \gamma_{43}^c r_i^4 Z_{43}(\theta_i, \varphi_i) + \gamma_{43}^s r_i^4 Z_{43}^s(\theta_i, \varphi_i), \end{aligned} \tag{4}$$

where r_i, θ_i and φ_i are spherical coordinates of the i-th electron. The Zeeman operator can be written by the parallel or perpendicular component to the C_3 axis as follows:

$$\hat{H}_{\parallel} = \sum_i \mu_{\mathrm{B}} (k\hat{l}_{iz} + g_{\mathrm{e}} \hat{s}_{iz}) \cdot H_z, \tag{5}$$

$$\hat{H}_{\perp} = \sum_i \mu_{\mathrm{B}} (k\hat{l}_{ix} + g_{\mathrm{e}} \hat{s}_{ix}) \cdot H_x. \tag{6}$$

Then, from (3) we establish the complete energy matrices in the trigonal ligand-field. The matrix elements can been expressed as functions of the Racah parameters B and C, the spin-orbit coupling coefficient ζ and the ligand-field parameters B_{20}, B_{40}, B_{43}^c, B_{43}^s. Generally, the z-axis is chosen along the threefold axis. However, based on the point charge and superposition model, the ligand-field parameter B_{43}^s will vanish and B_{20}, B_{40}, B_{43}^c can be derived as [11]

$$\begin{aligned} B_{20} &= \frac{1}{2} \sum_\tau G_2(\tau)(3\cos^2\theta_\tau - 1), \\ B_{40} &= \frac{1}{8} \sum_\tau G_4(\tau)(35\cos^4\theta_\tau - 30\cos^2\theta_\tau + 3), \\ B_{43}^c &= \frac{\sqrt{35}}{4} \sum_\tau G_4(\tau)(\cos\theta_\tau \sin^3\theta_\tau \cos 3\phi_\tau), \end{aligned} \tag{7}$$

where $G_2(\tau)$ and $G_4(\tau)$ are written as

$$\begin{aligned} G_2(\tau) &= -q_\tau e G^2(\tau), \\ G_4(\tau) &= -q_\tau e G^4(\tau), \\ G^k(\tau) &= \int_0^{R_\tau} R_{3\mathrm{d}}^2(r) r^2 \frac{r^k}{R_\tau^{k+1}} \mathrm{d}r \\ &\quad + \int_{R_\tau}^{\infty} R_{3\mathrm{d}}^2(r) r^2 \frac{R_\tau^k}{r^{k+1}} \mathrm{d}r. \end{aligned} \tag{8}$$

τ and q_τ represent the τ-th ligand and its effective charge, respectively, R_τ in (8) represents the Ni-$\mathrm{H_2O}$ bond length and θ_τ in (7) the angle between the Ni-$\mathrm{H_2O}$ bond and the C_3 axis. According to the Van Vleck approximation for the $G^k(\tau)$ integral [12], we obtain the relations

$$G_2(\tau) = \frac{A_2}{R_\tau^3}, \quad G_4(\tau) = \frac{A_4}{R_\tau^5}, \tag{9}$$

where $A_4 = -eq_\tau \langle r^4 \rangle$, $A_2 = -eq_\tau \langle r^2 \rangle$, $A_2/A_4 = \langle r^2 \rangle / \langle r^4 \rangle$. In the previous works, the radial wave function of Ni^{2+} has been given [13], and the crystal structure and optical spectra of $\mathrm{NiSiF_6 \cdot 6H_2O}$ have been reported [14, 15], from which we can derive $\langle r^2 \rangle / \langle r^4 \rangle = 0.141029$, $A_4 = 20.9$ a. u. and $A_2 = 2.9475$ a. u. for the $[\mathrm{Ni(H_2O)_6}]^{2+}$ cluster. According to Curie et al.'s covalence theory [16], the covalence factor N can be used to describe the Racah parameters B and C and the spin-orbit coupling coefficient ζ as follows:

$$B = N^4 B_0, \quad C = N^4 C_0, \quad \zeta = N^2 \zeta_0, \tag{10}$$

where $B_0 = 1084\ \mathrm{cm}^{-1}$, $C_0 = 4831\ \mathrm{cm}^{-1}$, $\zeta_0 = 649\ \mathrm{cm}^{-1}$ are the free-ion parameters [17]. Then, by diagonalizing the complete energy matrices, the interrelation between electronic and molecular structure may be established, and the local structure of the octahedral $[\mathrm{Ni(H_2O)_6}]^{2+}$ cluster in $\mathrm{NiTiF_6 \cdot 6H_2O}$ and $\mathrm{ZnSiF_6 \cdot 6H_2O}$ crystals can be determined by analyzing the EPR and optical spectra.

3. Calculations of the Local Structure of Ni^{2+} in $\mathrm{NiTiF_6 \cdot 6H_2O}$ and $\mathrm{ZnSiF_6 \cdot 6H_2O}$

The $\mathrm{NiTiF_6 \cdot 6H_2O}$ and $\mathrm{ZnSiF_6 \cdot 6H_2O}$ crystals are two of the series of isomorphous compounds. The Ni^{2+} (Zn^{2+}) ion is surrounded by six water molecules. When considering the Ni^{2+} ion in $\mathrm{NiTiF_6 \cdot 6H_2O}$ and $\mathrm{ZnSiF_6 \cdot 6H_2O}$ crystals, the local lattice structure of the octahedral Ni^{2+} centre is similar to that of

Table 1. The ZFS parameters D and $g_\parallel$, $g_\perp$ for $NiTiF_6 \cdot 6H_2O$:Ni^{2+} at 4.2, 77 and 298 K.

T (K)	R (Å)	$\Delta\theta$ (°)	$-D$ (cm^{-1})	$g_\parallel$	$g_\perp$
4.2	2.0325	0.3945	1.2407	2.2590	2.2489
		0.4045	1.2715	2.2592	2.2488
		0.4144	**1.3020**	**2.2593**	**2.2487**
		0.4245	1.3331	2.2595	2.2486
		0.4345	1.3639	2.2597	2.2486
Expt. [2]			**1.3 ± 0.01**	**2.27 ± 0.02**	**2.25 ± 0.02**
77	2.0338	0.4045	1.2775	2.2599	2.2495
		0.4145	1.3085	2.2601	2.2495
		0.4238	**1.3372**	**2.2603**	**2.2494**
		0.4345	1.3703	2.2604	2.2493
		0.4445	1.4012	2.2606	2.2492
Expt. [2]			**1.337 ± 0.006**	**2.27 ± 0.02**	**2.26 ± 0.02**
298	2.0543	0.3745	1.2741	2.2718	2.2616
		0.3845	1.3075	2.2720	2.2615
		0.3854	**1.3105**	**2.2720**	**2.2614**
		0.3945	1.3409	2.2722	2.2614
		0.4045	1.3743	2.2724	2.2613
Expt. [2]			**1.31 ± 0.01**	**2.28 ± 0.02**	**2.27 ± 0.02**

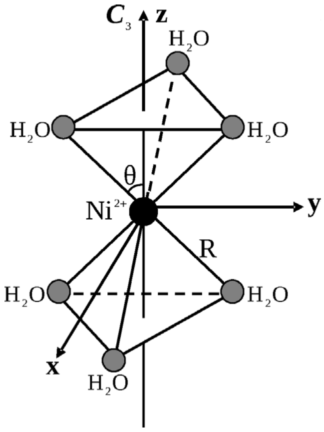

Fig. 1. The local structure of a Ni^{2+} centre in $NiTiF_6 \cdot 6H_2O$ and $ZnSiF_6 \cdot 6H_2O$. The Ni^{2+} ion is surrounded by six water molecules. R is the Ni-H_2O bond length and θ is the angle between the Ni-H_2O bond and the C_3 axis.

$NiSiF_6 \cdot 6H_2O$. As for the $ZnSiF_6 \cdot 6H_2O$:Ni^{2+} system, the Ni^{2+} ion will occupy the Zn^{2+} site, that is surrounded by six neighbour H_2O molecules. The local structure symmetry around Ni^{2+} in $NiTiF_6 \cdot 6H_2O$ and $ZnSiF_6 \cdot 6H_2O$ crystals belongs to the $R\bar{3}$ space group. The Ni^{2+} ion is surrounded by six water molecules which make an octahedron along the C_3 axis. In order to describe the local lattice structure of the octahedral $[Ni(H_2O)_6]^{2+}$ cluster in $NiTiF_6 \cdot 6H_2O$ and $ZnSiF_6 \cdot 6H_2O$ crystals, we introduce the two local structure parameters R and θ, which denote the Ni-H_2O bond length and the angle between Ni-H_2O bond and C_3 axis, respectively, as plotted in Figure 1. As for the $NiTiF_6 \cdot 6H_2O$:Ni^{2+} and $ZnSiF_6 \cdot 6H_2O$:Ni^{2+} systems, they have a similar crystal structure and the same type of ligand in $NiSiF_6 \cdot 6H_2O$, so it is reasonable to approximately apply the optical spectra of $NiSiF_6 \cdot 6H_2O$ to our calculation. In this case we obtain $R = 2.0325$ Å, 2.0338 Å, and 2.0543 Å for $NiTiF_6 \cdot 6H_2O$ and $R = 2.0327$ Å, 2.0341 Å, and 2.0481 Å for $ZnSiF_6 \cdot 6H_2O$:Ni^{2+} at 4.2, 77 and 298 (302) K. Meanwhile, $N = 0.969$ is obtained and $k \approx N^2$ can also be evaluated. The local structure parameter θ for the octahedral $[Ni(H_2O)_6]^{2+}$ cluster in $NiTiF_6 \cdot 6H_2O$ and $ZnSiF_6 \cdot 6H_2O$ can be expressed as

$$\theta = \theta_{oh} + \Delta\theta, \qquad (11)$$

where θ_{oh} denotes the bond angle between the Ni-H_2O (Zn-H_2O) bond and the C_3 axis of $NiTiF_6 \cdot 6H_2O$ ($ZnSiF_6 \cdot 6H_2O$) in the cubic symmetry [$\theta_{oh} = \cos^{-1}(1/\sqrt{3}) \approx 54.7356°$] [18]. $\Delta\theta$ represents trigonal distortion. Then, in the complete energy matrices, the trigonal distortion angle $\Delta\theta$ is the only adjustable parameter for Ni^{2+} in $NiTiF_6 \cdot 6H_2O$ and $ZnSiF_6 \cdot 6H_2O$:Ni^{2+} systems. It can be obtained by fitting the calculated zero-field splitting parameter D and g factors to the observed values. The results are listed in Tables 1 and 2. From our calculation, the EPR parameters (in particular the ZFS parameter D) depend strongly on the change of the bond angle and are not sensitive to the small change of the local structure parameter R. Simultaneously, the optical spectra of Ni^{2+} in $NiTiF_6 \cdot 6H_2O$ and $ZnSiF_6 \cdot 6H_2O$ are listed in Table 3; they are close to each other.

From Tables 1 – 3, by simulating the EPR and optical spectra, the values of $R = 2.0325$ Å, $\Delta\theta = 0.4144°$;

Table 2. The ZFS parameters D and $g_{\parallel}$, $g_{\perp}$ for $ZnSiF_6 \cdot 6H_2O$:Ni^{2+} at 4.2, 77 and 302 K.

T (K)	R (Å)	$\Delta\theta$ (°)	$-D$ (cm^{-1})	$g_{\parallel}$	$g_{\perp}$
4.2	2.0327	0.0244	0.0781	2.2328	2.2325
		0.0344	0.1100	2.2329	2.2317
		0.0414	**0.1324**	**2.2330**	**2.2321**
		0.0544	0.1739	2.2332	2.2321
Expt.			**0.1325±0.001** [5]	**2.233±0.002** [5]	**2.24±0.01***
			0.129 ±0.001 [6]	**2.25±0.01** [6]	
77	2.0341	0.0444	0.1427	2.2338	2.2329
		0.0544	0.1748	2.2340	2.2327
		0.0593	**0.1905**	**2.2341**	**2.2326**
		0.0644	0.2068	2.2342	2.2327
Expt.			**0.1905±0.0015** [5]	**2.235±0.005** [5]	
			0.2±0.01 [6]	**2.25±0.01** [6]	
			0.191±0.002 [7]	**2.23±0.01** [7]	
302	2.0481	0.1744	0.5857	2.2590	2.2544
		0.1844	0.6190	2.2592	2.2543
		0.1907	**0.6400**	**2.2593**	**2.2543**
		0.2044	0.6855	2.2595	2.2541
Expt.			**0.64±0.01** [5]	**2.26±0.02** [5]	**2.25±0.02***

* Obtained from $NiSiF_6 \cdot 6H_2O$ in [19].

Table 3. The observed and calculated optical spectral data of Ni^{2+} in the two crystals $NiTiF_6 \cdot 6H_2O$ (A) and $ZnSiF_6 \cdot 6H_2O$ (B) at 4.2, 77 and 298 (302) K; $N = 0.969$; all units in cm^{-1}.

	4.2 K			77 K			298 K		
Level	Calc.		Obs.[a]	Calc.		Obs.[a]	Calc.		Obs.[a]
	A	B		A	B		A	B[b]	
$^3T_2(^3F)$	9074	9161	9150	9043	9127	9120	8605	8796	8800
	9182	9172		9153	9143		8703	8845	
$^3T_1(^3F)$	15080	15173		15035	15124		14381	14646	14800
	15281	15193	15400	15240	15152	15290	14558	14735	
$^1E(^1D)$	15609	15612		15608	15610		15582	15593	
$^1T_2(^1D)$	24178	24333		24143	24293		23679	23916	
	24387	24353		24356	24322		23865	24008	
$^1A_1(^1G)$	25127	25124	24450	25117	25113		24942	24998	
$^3T_1(^3P)$	26277	26627	26100	26226	26564	26000	25594	25988	25650
	26804	26680		26763	26639		26067	26226	

[a] Spectral data obtained from [15].
[b] At 302 K.

$R = 2.0338$ Å, $\Delta\theta = 0.4238°$; and $R = 2.0543$ Å, $\Delta\theta = 0.3854°$ for Ni^{2+} in $NiTiF_6 \cdot 6H_2O$ and $R = 2.0327$ Å, $\Delta\theta = 0.0414°$; $R = 2.0341$ Å, $\Delta\theta = 0.0593°$; and $R = 2.0481$ Å, $\Delta\theta = 0.1907°$ for Ni^{2+} in $ZnSiF_6 \cdot 6H_2O$ are determined at 4.2, 77 and 298 (302) K, respectively. Simultaneously, we can determine the local structure parameters $R = 2.0325$ Å, $\theta = 55.1500°$; $R = 2.0338$ Å, $\theta = 55.1594°$; and $R = 2.0543$ Å, $\theta = 55.1210°$ for Ni^{2+} in $NiTiF_6 \cdot 6H_2O$ and $R = 2.0327$ Å, $\theta = 54.7770°$; $R = 2.0341$ Å, $\theta = 54.7949°$; and $R = 2.0481$ Å, $\theta = 54.9263°$ for Ni^{2+} in $ZnSiF_6 \cdot 6H_2O$ at temperatures 4.2, 77 and 298 (302) K, respectively. It must be pointed out that, due to the influence of H^+ ions, the calculated local structure parameters R and θ are at the equivalent position to the effective charge of the H_2O molecule rather than that of the O^{2-} ion. According to the former theoretical and experimental researches, $\theta < \theta_{oh}$ represents the local lattice structure of the 3d^n cations in trigonal crystals exhibiting an elongation distortion, contrarily, $\theta > \theta_{oh}$ represents the local lattice structure of the 3d^n cations in trigonal crystals exhibiting a compression distortion. The results of Tables 1 and 2 show that the local lattice structure around the Ni^{2+} centre in $NiTiF_6 \cdot 6H_2O$ and $ZnSiF_6 \cdot 6H_2O$ has a compression distortion. Furthermore, the local lattice distortion degree for Ni^{2+} in $ZnSiF_6 \cdot 6H_2O$ increases with rising temperature, whereas for Ni^{2+} in $NiTiF_6 \cdot 6H_2O$ the angle distortion degree at 77 K is larger than at 4.2 K and 298 K. This exceptional variation for $NiTiF_6 \cdot 6H_2O$ may be ascribed to the fact that the ZFS parameter D is very sensitive to the local structure parameter θ, and the values of $|D|$ observed in the experiment increase with temperature up to about 77 K, then decrease between about 77 K and 298 K.

4. Study of the Relationship between the Orbital Reduction Factor *k* and the *g* Factors

From (3), the orbital reduction factor k is taken into account for the Zeeman interaction in the perturbation Hamiltonian. By using the corresponding pa-

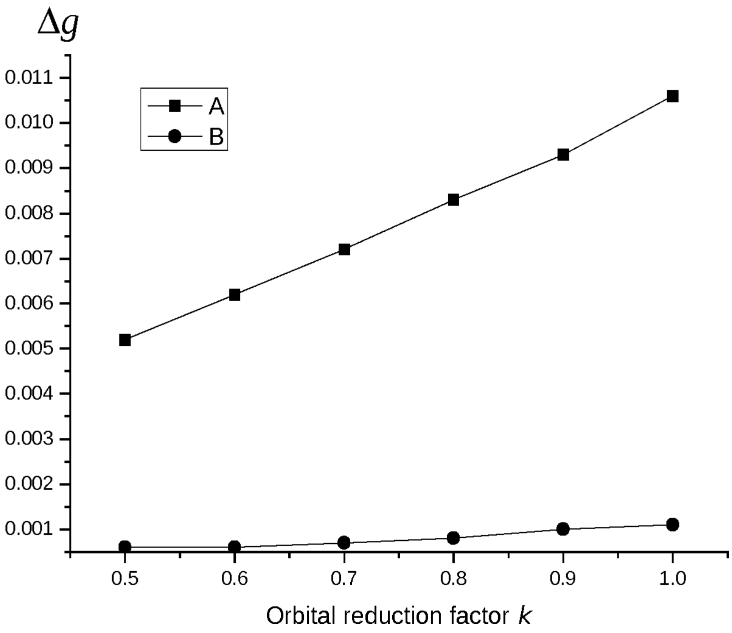

Fig. 2. The relationship between Δg and the orbital reduction factor k for $NiTiF_6 \cdot 6H_2O:Ni^{2+}$ (A) and $ZnSiF_6 \cdot 6H_2O:Ni^{2+}$ (B) at 4.2 K.

Table 4. The relationship between the EPR g factors and the orbital reduction factor k for $NiTiF_6 \cdot 6H_2O:Ni^{2+}$ at 4.2, 77 and 298 K.

	4.2 K		77 K		298 K	
k	$g_\parallel$	$g_\perp$	$g_\parallel$	$g_\perp$	$g_\parallel$	$g_\perp$
0.5	2.1262	2.1210	2.1266	2.1210	2.1321	2.1267
0.6	2.1528	2.1466	2.1534	2.1467	2.1601	2.1536
0.7	2.1794	2.1722	2.1801	2.1724	2.1881	2.1806
0.8	2.2061	2.1978	2.2068	2.1980	2.2160	2.2075
0.9	2.2327	2.2234	2.2335	2.2237	2.2440	2.2345
1.0	2.2593	2.2487	2.2603	2.2494	2.2720	2.2614

Table 5. The relationship between the EPR g factors and the orbital reduction factor k for $ZnSiF_6 \cdot 6H_2O:Ni^{2+}$ at 4.2, 77 and 302 K.

	4.2 K		77 K		302 K	
k	$g_\parallel$	$g_\perp$	$g_\parallel$	$g_\perp$	$g_\parallel$	$g_\perp$
0.5	2.1230	2.1224	2.1235	2.1230	2.1285	2.1259
0.6	2.1490	2.1484	2.1497	2.1490	2.1558	2.1527
0.7	2.1750	2.1743	2.1758	2.1750	2.1830	2.1794
0.8	2.2010	2.2002	2.2019	2.2009	2.2103	2.2062
0.9	2.2271	2.2261	2.2281	2.2269	2.2375	2.2329
1.0	2.2531	2.2520	2.2542	2.2529	2.2648	2.2597

rameters at different temperatures above and adjusting the orbital reduction factor, the EPR parameters are determined depending on different k for Ni^{2+} in $NiTiF_6 \cdot 6H_2O$ and $ZnSiF_6 \cdot 6H_2O$, which are listed in Tables 4 and 5. Meanwhile, the relationship between Δg $(= g_\parallel - g_\perp)$ and the orbital reduction factor k for Ni^{2+} in $NiTiF_6 \cdot 6H_2O$ and $ZnSiF_6 \cdot 6H_2O$ at different temperatures is plotted in Figures 2 – 4. From Tables 4 and 5 we can see that both $g_\parallel$ and $g_\perp$ for the two systems increase obviously when the orbital reduction factor k increases. From Figs. 2 – 4, it is shown that: (i) Δg is positive at all values of k with a magnitude that increases monotonically with the orbital reduction factor k. Generally, the sign of Δg is related to the ZFS parameter D; for a d^8 ion under the weak field approximation, the sign of Δg is contrary to that of the ZFS parameter D. Hence, for Ni^{2+} in $NiTiF_6 \cdot 6H_2O$ and $ZnSiF_6 \cdot 6H_2O$ crystals, the value of $g_\parallel$ is larger than that of $g_\perp$, which corresponds to the negative ZFS parameter D. (ii) At each temperature, there is an almost linear relation between k and Δg for Ni^{2+} in $NiTiF_6 \cdot 6H_2O$ and $ZnSiF_6 \cdot 6H_2O$.

5. Conclusion

By diagonalizing the complete energy matrices, the local structure parameters and the zero-field splitting parameter D as well as the g factors of $NiTiF_6 \cdot 6H_2O$ and $ZnSiF_6 \cdot 6H_2O:Ni^{2+}$have been studied at different temperatures. It has been shown that the local lattice structure around the octahedral Ni^{2+} centre in $NiTiF_6 \cdot 6H_2O$ and $ZnSiF_6 \cdot 6H_2O$ exhibits a compression distortion. The angle distortion degree of $NiTiF_6 \cdot 6H_2O$ at 77 K is larger than that at 4.2 K and 298 K. For the $ZnSiF_6 \cdot 6H_2O:Ni^{2+}$ system, the compression distortion may be ascribed to the fact that

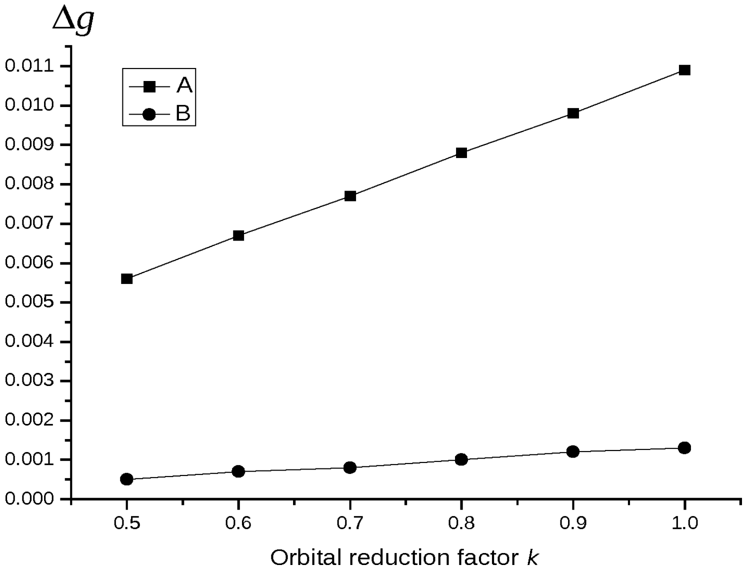

Fig. 3. The relationship between Δg and the orbital reduction factor k for $\mathrm{NiTiF_6 \cdot 6H_2O{:}Ni^{2+}}$ (A) and $\mathrm{ZnSiF_6 \cdot 6H_2O{:}Ni^{2+}}$ (B) at 77 K.

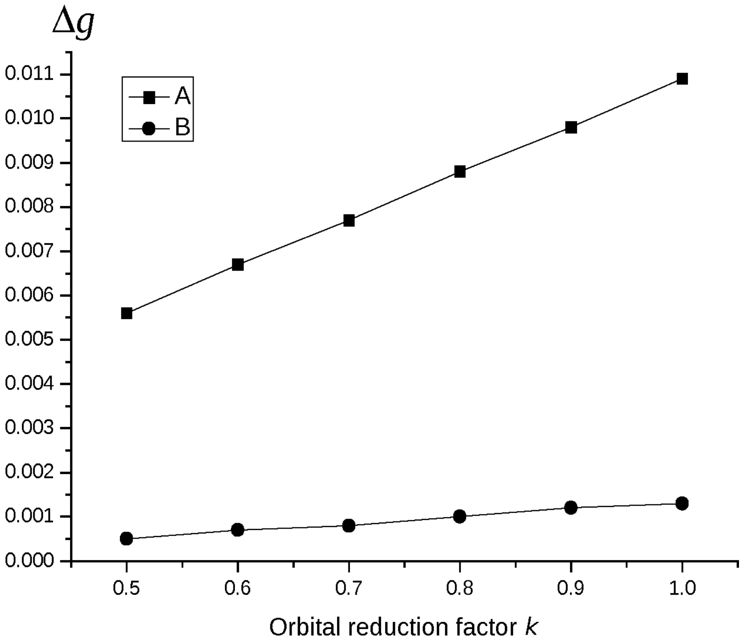

Fig. 4. The relationship between Δg and the orbital reduction factor k for $\mathrm{NiTiF_6 \cdot 6H_2O{:}Ni^{2+}}$ (A) and $\mathrm{ZnSiF_6 \cdot 6H_2O{:}Ni^{2+}}$ (B) at room temperature.

the radius of the $\mathrm{Ni^{2+}}$ ion (0.72 Å) is smaller than that of the host ion $\mathrm{Zn^{2+}}$ (0.75 Å) and the local lattice distortion degree of $\mathrm{Ni^{2+}}$ in $\mathrm{ZnSiF_6 \cdot 6H_2O}$ increases with rising temperature. In addition, from our calculation, we also found that the EPR g factors $g_{\parallel}$ and $g_{\perp}$ depend sensitively on the orbital reduction factor k and there is a nearly linear relation between k and Δg for $\mathrm{Ni^{2+}}$ in $\mathrm{NiTiF_6 \cdot 6H_2O}$ and $\mathrm{ZnSiF_6 \cdot 6H_2O}$ at each temperature.

Acknowledgement

This work was supported by the National Natural Science Foundation of China (No. 10774103) and the Doctoral Education Fund of the Education Ministry of China (No. 20050610011).

[1] L. Pauling, Z. Kristallogr. **72**, 482 (1930).

[2] R. S. Rubins, B. C. Griffin, and R. Burris, J. Chem. Phys. **64**, 3349 (1976).

[3] S. A. Al'tshuler and R. M. Valishev, Sov. Phys. JETP **21**, 309 (1965).

[4] R. S. Rubins, J. Chem. Phys. **84**, 4142 (1986).

[5] R. S. Rubins and S. K. Jani, J. Chem. Phys. **66**, 3297 (1977).

[6] R. H. Hoskins, R. C. Pastor, and K. R. Trigger, J. Chem. Phys. **30**, 601 (1959).

[7] I. J. Fritz and L. Yarmus, J. Chem. Phys. **51**, 1428 (1969).

[8] A. Abragam and B. Bleaney, Electron Paramagnetic Resonance of Transition Ions, Oxford University Press, Oxford 1970.

[9] X. Y. Kuang, Phys. Rev. B **36**, 712 (1987); B **36**, 797 (1987); X. Y. Kuang, Ph. D. Thesis, Université Paris-sud, 1994, p. 14.

[10] O. Kahn, Molecular Magnetism, VCH, New York 1993, p. 31.

[11] D. J. Newman and W. Urban, Adv. Phys. **24**, 793 (1975).

[12] J. H. VanVleck, J. Chem. Phys. **1**, 208 (1932).

[13] M. G. Zhao, M. L. Du, and G. Y. Sen, J. Phys. C: Solid State Phys. **20**, 5557 (1987).

[14] S. Ray, A. Zalkin, and D. H. Templeton, Acta Cryst. B **29**, 2741 (1973).

[15] M. H. L. Pryce, G. Agnetta, T. Garofano, M. B. Paima-Vittorelli, and M. U. Palma, Phil. Mag. **10**, 477 (1964).

[16] D. Curie, C. Barthon, and B. Canny, J. Chem. Phys. **61**, 3048 (1974).

[17] J. S. Griffith, The Theory of Transition-Metal Ions, Cambridge University Press, London 1964.

[18] W. C. Zheng, Radiat. Eff. Defect Solids **140**, 329 (1997).

[19] R. S. Rubins, J. D. Clark, and S. K. Jani, J. Chem. Phys. **67**, 893 (1977).